Effects of Electron-Cyclotron-Resonance-Heating-Induced Internal Kink Mode on the Toroidal Rotation in the KSTAR Tokamak

J. Seol,[1] S. G. Lee,[1] B. H. Park,[1] H. H. Lee,[1] L. Terzolo,[1] K. C. Shaing,[2,3] K. I. You,[1] G. S. Yun,[4] C. C. Kim,[5] K. D. Lee,[1] W. H. Ko,[1] J. G. Kwak,[1] W. C. Kim,[1] Y. K. Oh,[1] J. Y. Kim,[1] S. S. Kim,[1] and K. Ida[6]

[1]*National Fusion Research Institute, Gwahangno 113, Yuseong-gu, Daejeon 305-333, Korea*
[2]*Institute for Space, Astrophysical and Plasma Sciences, National Cheng Kung University, Tainan, Taiwan 70101, Republic of China*
[3]*Engineering Physics Department, University of Wisconsin, Madison, Wisconsin 53706, USA*
[4]*POSTECH, Pohang 790-784, Korea*
[5]*FAR-TECH, Inc., San Diego, California 92121, USA*
[6]*National Institute for Fusion Science, Toki, 509-5292, Japan*

(Received 15 May 2012; published 8 November 2012)

It is observed that the magnitude of the toroidal rotation speed is reduced by the central electron cyclotron resonance heating (ECRH) regardless of the direction of the toroidal rotation. The magnetohydrodynamics activities generally appear with the rotation change due to ECRH. It is shown that the internal kink mode is induced by the central ECRH and breaks the toroidal symmetry. When the magnetohydrodynamics activities are present, the toroidal plasma viscosity is not negligible. The observed effects of ECRH on the toroidal plasma rotation are explained by the neoclassical toroidal viscosity in this Letter. It is found that the neoclassical toroidal viscosity torque caused by the internal kink mode damps the toroidal rotation.

DOI: 10.1103/PhysRevLett.109.195003 PACS numbers: 52.55.Fa, 52.50.Sw, 52.55.Dy

Toroidal plasma rotation in a tokamak has attracted a great deal of interest because of its effect on plasma stability and confinement. Toroidal rotation without external torques has been measured in many tokamaks [1]. Recently, the torque balance between various sources and sinks has been studied theoretically with relevant boundary conditions [2].

Toroidal rotation changes due to electron cyclotron resonance heating have been measured in many devices. However, there is no widely accepted explanation for the effects of electron cyclotron resonance heating (ECRH) on the toroidal rotation. In this Letter, we introduce the results of the KSTAR tokamak [3] on the toroidal rotation changes induced by the central electron cyclotron resonance heating, which is used for many purposes such as heating, current drive, and sawtooth control [4–7]. In KSTAR, the central heating is more efficient on the rotation change than heating on the outer region of the plasmas. Toroidal rotation changes are generally larger in the core plasmas. The toroidal rotation is reduced indicating that countercurrent directed torque is generated by electron cyclotron resonance heating in the cocurrent directed rotating plasmas. On the other hand, the toroidal rotation in the countercurrent directed rotating plasmas changes in the opposite way showing that electron cyclotron resonance heating causes the cocurrent directed torque. Both in the cocurrent and the countercurrent directed rotating plasmas, the magnitude of the toroidal rotation is reduced when electron cyclotron resonance heating is applied. In addition, magnetohydrodynamics (MHD) activities appear very often with the rotation changes. Similar phenomena with the KSTAR results have also been observed in other devices such as DIII-D [8–10], JT-60U [11,12], ASDEX-Upgrade [13], and TEXTOR [14].

Previously, $m = 1, n = 1$ mode has been observed when the central ECRH was injected in DIII-D [15], HL-1M [16], and ASDEX Upgrade [13]. In the KSTAR tokamak, internal kink modes generally appear with the central ECRH injection. When MHD activities are present in the tokamak, the toroidal symmetry is broken. In this case, the neoclassical toroidal viscosity (NTV) is not negligible any more [17]. The toroidal flow damping rate can be enhanced significantly by the neoclassical toroidal viscosity caused by MHD activities. Thus, the neoclassical toroidal viscosity needs to be considered when the effects of ECRH on the toroidal rotation is investigated. In this research, it is shown that the effects of ECRH on the toroidal rotation can be explained by the toroidal flow damping caused by the neoclassical toroidal viscosity. The magnetic field perturbation δB caused by ECRH-induced internal kink modes is estimated from the measured plasma displacement profile. The NTV torque density is estimated using δB to give a comparison with the neutral beam injection (NBI) torque density when the toroidal rotation evolution goes to the steady state.

The experiment is conducted both in NBI heated plasmas and Ohmic heated plasmas. The microwave beam is injected perpendicularly for on-axis ECRH during the flattop phase in both cases. The argon impurity toroidal rotation is measured via an x-ray imaging crystal spectrometer (XCS) and the carbon impurity rotation by charge exchange spectroscopy (CES). The core toroidal rotation

measurement by XCS and CES agrees well with the MHD frequency measurement of the sawtooth precursors located inside the inversion radius. In the KSTAR tokamak, the Ohmic heated plasmas without external torques generally rotate in the countercurrent direction. The magnitude of the toroidal rotation is reduced when ECRH is injected in the Ohmic heated plasmas ($R = 1.8$ m, $a = 0.5$ m, $\kappa = 1.15$, $q_{95} = 6.0$, $I_p = 0.6$ MA, $B_t = 1.96$ T) while the plasma is still rotating in the countercurrent direction as shown in Fig. 1. Figure 1 shows that the toroidal rotation is reduced during ECRH injection and recovered when ECRH is turned off. The NBI heated plasmas in the KSTAR tokamak rotate in the cocurrent direction because of a strong cocurrent directed momentum source from NBI. As it is shown in Fig. 2, the ECRH injection reduces the toroidal rotation of the NBI heated plasmas ($R = 1.81$ m, $a = 0.48$ m, $\kappa = 1.81$, $q_{95} = 6.5$, $I_p = 0.6$ MA, $B_t = 1.96$ T). The toroidal rotation reduction starts inside the sawtooth inversion radius in the beginning. On the other hand, the toroidal rotation increases outside the sawtooth inversion radius at the same time. The toroidal rotation decreases gradually until $t = 3.935$ and goes to the steady state. Figures 1 and 2 clearly show that the central ECRH reduces the magnitude of the toroidal rotation regardless of the rotation direction rather than cocurrent or countercurrent directed torques.

The kinklike modes are observed inside the inversion radius in almost all discharges when ECRH is injected in the core. As shown in Fig. 3, the internal kink mode appears with the central injection of ECRH. The electron temperature profiles are obtained from the high field side electron cyclotron emission (ECE) measurement. The internal kink boundary coincides with the sawtooth inversion radius, which can be considered as an approximate $q = 1$ surface. It seems that the kink mode driven by ECRH is due to interactions between energetic electrons generated by ECRH and an $m = 1$, $n = 1$ mode [15,16]. The kink instabilities appear only when ECRH is turned on and disappear when ECRH is turned off. Note that the kink instabilities are generally accompanied by the sawtooth oscillations. However, the internal kink modes appear right after the sawtooth collapse and stay until the next sawtooth collapse. It implies that the internal kink mode resides for most of the time period in which ECRH is injected, while the kink-tearing mode for the typical sawtooth collapse resides only for a relatively short time. In recent theoretical study [18], it has been shown that energetic ions can destabilize the kink mode even when the safety factor q is slightly larger than 1. Energetic electrons may also be able to destabilize the internal kink mode near $q = 1$ surface. The magnetic field perturbation due to the internal kink mode can induce the parallel viscosity in the toroidal direction. Finally, the toroidal rotation can be damped toward the steady state toroidal rotation [17].

Recently, the NTV theory has been developed by solving the drift kinetic equation in the different collisionality regimes [19–21]. An approximate analytic expression connecting the formula in different collisionality regimes has been obtained by rational approximation [22]. Another

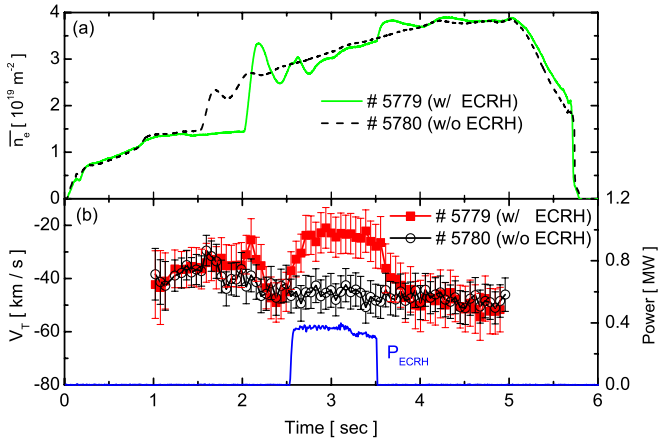

FIG. 1 (color online). (a) The line integrated plasma densities ($\bar{n}_e$) for Ohmic heated discharges with (solid line) and without (dashed line) ECRH. (b) The time traces of the core toroidal rotation speed (V_T) for Ohmic heated discharges with (square) and without (circle) ECRH, measured by XCS. 400 kW on-axis ECRH is injected at $t = 2.5$–3.5 s for shot 5779.

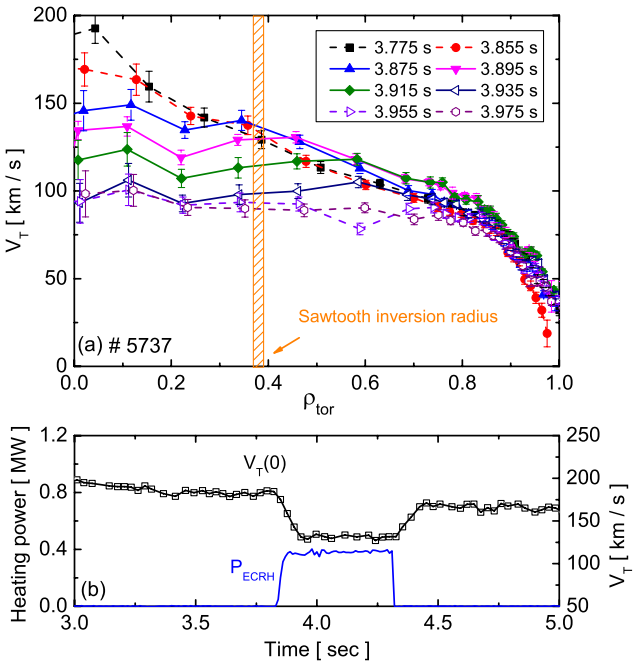

FIG. 2 (color online). (a) Toroidal rotation profiles for shot 5737 measured by CES. 350 kW on-axis ECRH injection at $t = 3.84$–4.3 s in the NBI heated plasma rotating in the cocurrent direction. The onset of the internal kink mode is at $t \approx 3.85$ s. The rotation profiles are presented with a 20 ms time intervals during ECRH injection while with an 80 ms time interval before ECRH injection. (b) The time trace of the core toroidal rotation speed for shot 5737 measured by XCS.

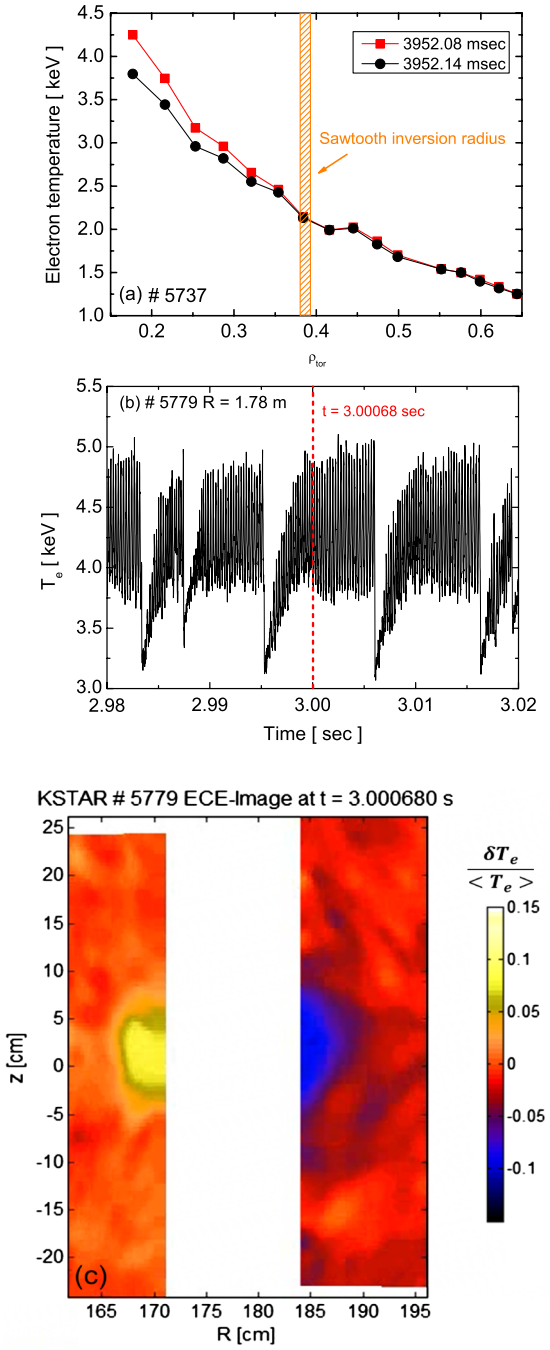

FIG. 3 (color online). (a) Electron temperature profiles from the ECE measurements when the internal kink mode occurs for shot 5737 at $t = 3970.35$ ms and 3970.40 ms, separated by half the period. The electron temperature profile shifts only inside the sawtooth inversion radius. (b) Time trace of an ECE channel for shot 5779. (c) Electron cyclotron emission imaging data at $t = 3.00\,068$ s [indicated by the dashed line in (b)] show the internal kink mode for shot 5779. Here, $\langle T_e \rangle$ denotes a time average and $\delta T_e \equiv T_e - \langle T_e \rangle$.

treatment has been introduced by using the Krook collision operator to obtain a generalized analytic solution [23]. The NTV has been calculated also by numerical calculation [24,25]. Experimental observations have validated the NTV braking effect due to applied nonaxisymmetric magnetic fields [26,27] and MHD instabilities [28]. In this Letter, we calculate the NTV due to internal kink modes by using the methods introduced in Refs. [17,19]. The magnetic field strength in the presence of MHD activities can be expressed as

$$B = B_0(1 - \epsilon\cos\theta) - B_0\sum_n [A_n(\theta)\cos(n\zeta_0) + B_n(\theta)\sin(n\zeta_0)], \quad (1)$$

where B_0 is the magnetic field strength on the magnetic axis, $\epsilon \simeq r/R$, θ is the poloidal angle, ζ is the toroidal angle, $\zeta_0 = q\theta - \zeta$, q is the safety factor, n is the toroidal mode number, and $A_n(\theta)$ and $B_n(\theta)$ are the amplitudes of the $\cos(n\zeta_0)$ and $\sin(n\zeta_0)$, respectively. When a large radial electric field is present, $1/\nu$ regime or $\sqrt{\nu}$ regime is dominant depending on $\nu_E = (\nu/\epsilon)/q\omega_E$, where $\omega_E = E_r/rB_t$ is the $\mathbf{E} \times \mathbf{B}$ drift frequency. The collision frequency ν is defined as $\nu_i = \sqrt{2}\pi N_i e_i^4 \ln\Lambda/(M_i^{1/2}T_i^{3/2})$ for ions, and $\nu_e = \sqrt{2}\pi N_i e_i^2 e_e^2 \ln\Lambda/(M_e^{1/2}T_e^{3/2})$ for electrons, where $\ln\Lambda$ is the Coulomb logarithm, N is the plasma density of species, T is the plasma temperature of species, M is the mass, and e_a is the charge of the species a. When $\nu_E < 1$ or $\nu_E > 1$, the plasma is in the $\sqrt{\nu}$ regime or the $1/\nu$ regime, respectively. The ion viscosity is larger than the electron viscosity by a factor of the order of $(M_i/M_e)^{1/2}$ when the plasma is in the $1/\nu$ regime. Ignoring the electron plasma viscosity, the NTV torque density in the $1/\nu$ regime can be written as [17]

$$T_{1/\nu} \simeq 6.1 N_i M_i v_{ti}^2 \frac{\epsilon^{3/2}}{\nu_i} n^2 \left(\frac{A_n^2 + B_n^2}{B_0^2}\right) \times \left\{V^\zeta - q\left(V^\theta + 2.367\frac{1}{erB_0}\frac{\partial T_i}{\partial r}\right)\right\}, \quad (2)$$

where v_{ti} is the thermal speed of ion, and $V^\zeta = \mathbf{V}\cdot\nabla\zeta$, $V^\theta = \mathbf{V}\cdot\nabla\theta$. When ions are slightly in the $\sqrt{\nu}$ regime and electrons are well in the $1/\nu$ regime, the ion viscosity is still much larger than the electron viscosity. The NTV torque density in the $\sqrt{\nu}$ regime can be written as [19]

$$T_{\sqrt{\nu}} \simeq 0.09 N_i M_i v_{ti}^2 \sqrt{\epsilon}\sqrt{\nu_E}\{\ln(8/\sqrt{\nu_{Ei}})\}^{1/2} n^2 \left(\frac{A_n^2 + B_n^2}{B_0^2}\right) \times \left\{V^\zeta - q\left(V^\theta + 0.356\frac{1}{erB_0}\frac{\partial T_i}{\partial r}\right)\right\}/q\omega_{Ei}, \quad (3)$$

where $\nu_{Ei} \equiv \frac{\nu_i/\epsilon}{q\omega_E}$. Figure 3 indicates that the plasma inside the sawtooth inversion radius shifts radially during ECRH injection. The plasma displacement ξ is obtained from the electron temperature profiles at two different times separated by half the period of the internal kink mode (shown in Fig. 3). The plasma displacement ξ by the kink mode is used to estimate the modification on B. For $m = 1$, $n = 1$ mode, $(\delta B/B) = (A_1^2 + B_1^2)^{1/2}/B_0 \approx (\xi/2)(1/B_0)\partial B/\partial r$. For the NBI-heated plasma discharge in the KSTAR

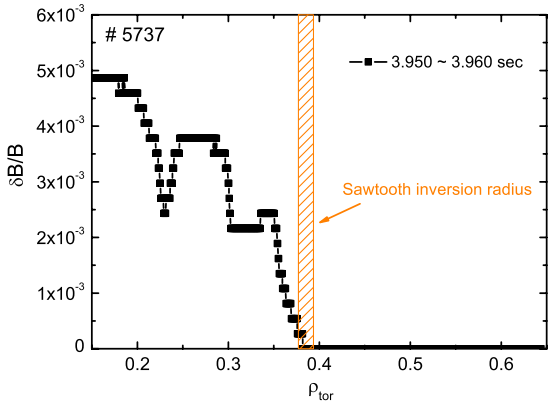

FIG. 4 (color online). Modification on B by the internal kink mode for shot 5737 at $t = 3.970$–3.980 s.

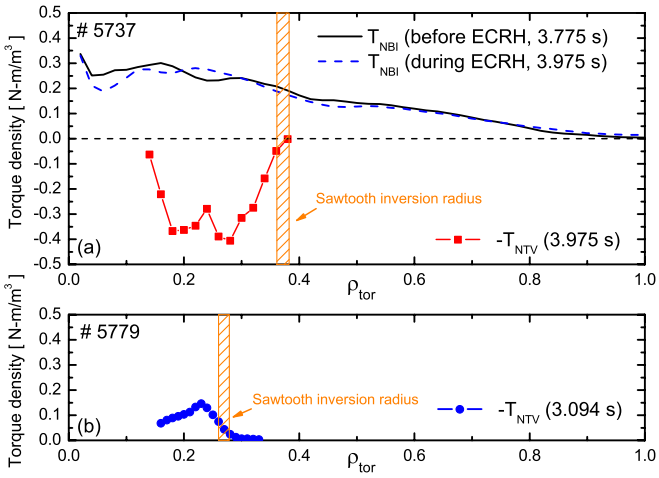

FIG. 5 (color online). (a) NBI torque density profiles (blue dashed line, black line) calculated by NUBEAM [30] and the NTV torque density profile calculated from the plasma displacement (red) when ECRH is injected in the NBI-heated H-mode plasma rotating in the cocurrent direction. Experimental profiles for shot 5737 at $t = 3.975$ s, are used to calculate the torque density profiles. (b) NTV torque density profile for shot 5779 when ECRH is injected in the Ohmic-heated plasma rotating in the countercurrent direction.

tokamak, the modification on B is of the order of $\delta B/B \sim 5 \times 10^{-3}$ as shown in Fig. 4. Finally, the toroidal plasma viscosity can be calculated using the magnetic field strength perturbation profile. The toroidal rotation in the presence of the MHD activities can be determined by the toroidal momentum balance equation [17]:

$$\frac{\partial \langle NM\mathbf{B}_t \cdot \mathbf{V} \rangle}{\partial t} = -\sum_j \langle \mathbf{B}_t \cdot \nabla \cdot \pi_j \rangle + S_M, \qquad (4)$$

where $\mathbf{B}_t$ is the toroidal component of $\mathbf{B}$, $\langle \mathbf{B}_t \cdot \nabla \cdot \pi \rangle$ is the toroidal component of the plasma viscosity, and S_M is the momentum sources or sinks. When the momentum sources are negligible, the toroidal flow is determined by

$$\sum_{j=i,e} \langle \mathbf{B}_t \cdot \nabla \cdot \pi_j \rangle = 0 \qquad (5)$$

in the steady state. The toroidal flow determined by Eq. (5) is the so-called steady state toroidal flow [17,29]. When the momentum sources are present, the NTV damps the toroidal flow until the NTV torque density is balanced with the toroidal torque sources. Equations (2) and (3) indicate that the magnitude of the NTV torque density generally decreases as the toroidal flow speed decreases, i.e., the NTV damps the toroidal rotation and decreases itself as well. After all, the toroidal flow speed is determined by $-T_{\mathrm{NTV}} + S_{\mathrm{torque}} = 0$ in the steady state when the momentum sources or sinks are present, where T_{NTV} is the NTV torque density and S_{torque} is the torque sources or sinks.

Figure 5 clearly shows that the NTV torque caused by the internal kink mode occurs inside the sawtooth inversion radius, which agrees with the toroidal flow evolution shown in Fig. 2. The NTV torque density profile can account for the toroidal rotation reduction in the core. The NTV torque density profile may also explain the temporal rotation increase outside the sawtooth inversion radius. The reduced toroidal momentum from the inside $q = 1$ surface can appear to the outside $q = 1$ surface temporally, which can go to the coils in the end. It is notable that the NTV torque density has its peak around $\rho_t = 0.2$–0.3. It also shows that the magnitude of the NTV torque density is similar to that of the NBI torque density in the core during the ECRH injection when the toroidal flow profile is saturated. In the steady state, the NTV torque density balances out the other momentum sources including the NBI torque. In the Ohmic heated discharges, the NTV torque also occurs inside the sawtooth inversion radius but in the cocurrent direction as shown in Fig. 5(b). The sign change of the NTV torque is due to the sign change of V_ζ in Eq. (2) or (3). It seems that the NTV torque, which is much smaller than the NBI torque, balances with the intrinsic momentum sources. Here, the NTV torque density is calculated using Eq. (2) since both ions and electrons are in the $1/\nu$ regime for the radial positions where $\xi \neq 0$.

In summary, toroidal rotation measurements in this study clearly show that the magnitude of the toroidal rotation is reduced both in the cocurrent and the countercurrent directed rotating plasmas when electron cyclotron resonance heating is injected in the core region. It is found that the internal kink mode appears with the central ECRH. The internal kink mode induced by ECRH results in the breaking of the toroidal symmetry and the corresponding NTV damping. Analysis shows that the the countercurrent directed NTV torque by the internal kink mode occurs in the cocurrent directed rotating plasmas, and vice versa. It also shows that the NTV torque is of the same order of magnitude with the NBI torque in the steady state. These agreements strongly suggest that the effects of the central ECRH on the toroidal rotation observed in many tokamaks

so far can be explained by the NTV damping caused by the internal kink mode.

The first two authors contributed equally to this work. This work was carried out within the framework of the KSTAR research project.

[1] J. E. Rice, A. Ince-Cushman, J. S. de Grassie, L.-G. Eriksson, Y. Sakamoto, A. Scarabosio, A. Bortolon, K. H. Burrell, B. P. Duval, C. Fenzi-Bonizec, M. J. Greenwald, R. J. Groebner, G. T. Hoang, Y. Koide, E. S. Marmar, A. Pochelon, and Y. Podpaly, Nucl. Fusion **47**, 1618 (2007).
[2] V. D. Pustovitov, Nucl. Fusion **51**, 013 006 (2011).
[3] M. Kwon *et al.*, (the KSTAR Team), Nucl. Fusion **51**, 094 006 (2011).
[4] C. Angioni, T. P. Goodman, M. A. Henderson, and O. Sauter, Nucl. Fusion **43**, 455 (2003).
[5] I. T. Chapman, Plasma Phys. Controlled Fusion **53**, 013 001 (2011).
[6] A Mück, T. P. Goodman, M. Maraschek, G. Pereverzev, F. Ryter, H. Zohm, and (the ASDEX Upgrade Team), Plasma Phys. Controlled Fusion **47**, 1633 (2005).
[7] A. Manini, J.-M. Moret, F. Ryter, and (the ASDEX Upgrade Team), Nucl. Fusion **43**, 490 (2003).
[8] J. S. de Grassie, C. M. Greenfield, D. R. Baker, K. H. Burrell, Y. R. Lin-Liu, J. Lohr, T. C. Luce, C. C. Petty, R. Prater, G. M. Staebler, W. W. Heidbrink, B. W. Rice, T. K. Mau, and M. Porkolab, in *Proceedings of the 26th EPS Conference on Controlled Fusion and Plasma Physics, Maastricht, 1999* (European Physical Society, Geneva, 1999), Vol. 23, p. 1189.
[9] J. S. de Grassie, K. H. Burrell, L. R. Baylor, W. Houlberg, and J. Lohr, Phys. Plasmas **11**, 4323 (2004).
[10] J. S. de Grassie, J. E. Rice, K. H. Burrell, R. J. Groebner, and W. M. Solomon, Phys. Plasmas **14**, 056 115 (2007).
[11] Y. Sakamoto, S. Ide, M. Yoshida, Y. Koide, T. Fujita, H. Takenaga, and Y. Kamada, Plasma Phys. Controlled Fusion **48**, A63 (2006).
[12] M. Yoshida, Y. Sakamoto, H. Takenaga, S. Ide, N. Oyama, T. Kobayashi, and Y. Kamada, Phys. Rev. Lett. **103**, 065003 (2009).
[13] R. M. McDermott, C. Angioni, R. Dux, A. Gude, T. Pütterich, F. Ryter, G. Tardini, and the ASDEX Upgrade Team, Plasma Phys. Controlled Fusion **53**, 035007 (2011).
[14] M. De Bock, PhD thesis, Technische Universiteit Eindhoven, 2007.
[15] K. L. Wong, M. S. Chu, T. C. Luce, C. C. Petty, P. A. Politzer, R. Prater, L. Chen, R. W. Harvey, M. E. Austin, L. C. Johnson, R. J. La Haye, and R. T. Snider, Phys. Rev. Lett. **85**, 996 (2000).
[16] X. T. Ding, Y. Liu, G. C. Guo, E. Y. Wang, K. L. Wong, L. W. Yan, J. Q. Dong, J. Y. Cao, Y. Zhou, J. Rao, Y. Yuan, H. Xia, Y. Liu, and (the HL-1M group), Nucl. Fusion **42**, 491 (2002).
[17] K. C. Shaing, Phys. Plasmas **10**, 1443 (2003).
[18] D. P. Brennan, C. C. Kim, and R. J. La Haye, Nucl. Fusion **52**, 033 004 (2012).
[19] K. C. Shaing, P. Cahyna, M. Becoulet, J.-K. Park, S. A. Sabbagh, and M. S. Chu, Phys. Plasmas **15**, 082 506 (2008).
[20] K. C. Shaing, S. A. Sabbagh, and M. S. Chu, Plasma Phys. Controlled Fusion **51**, 055 003 (2009).
[21] K. C. Shaing, S. A. Sabbagh, and M. S. Chu, Plasma Phys. Controlled Fusion **51**, 035 009 (2009).
[22] K. C. Shaing, J. Seol, Y. W. Sun, M. S. Chu, and S. A. Sabbagh, Nucl. Fusion **50**, 125 008 (2010).
[23] J. K. Park, A. H. Boozer, and J. E. Menard, Phys. Rev. Lett. **102**, 065002 (2009).
[24] Y. Sun, Y. Liang, K. C. Shaing, H. R. Koslowski, C. Wiegmann, and T. Zhang, Phys. Rev. Lett. **105**, 145002 (2010).
[25] S. Satake, J.-K. Park, H. Sugama, and R. Kanno, Phys. Rev. Lett. **107**, 055001 (2011).
[26] W. Zhu, S. A. Sabbagh, R. E. Bell, J. M. Bialek, M. G. Bell, B. P. LeBlanc, S. M. Kaye, F. M. Levinton, J. E. Menard, K. C. Shaing, A. C. Sontag, and H. Yuh, Phys. Rev. Lett. **96**, 225002 (2006).
[27] A. M. Garofalo, K. H. Burrell, J. C. De Boo, J. S. de Grassie, G. L. Jackson, M. Lanctot, H. Reimerdes, M. J. Schaffer, W. M. Solomon, and E. J. Strait, Phys. Rev. Lett. **101**, 195005 (2008).
[28] M.-D. Hua, I. T. Chapman, A. R. Field, R. J. Hastie, S. D. Pinches, and (the MAST Team), Plasma Phys. Controlled Fusion **52**, 035 009 (2010).
[29] M. S. Chu and M. Okabayashi, Plasma Phys. Controlled Fusion **52**, 123 001 (2010).
[30] A. Pankin, D. McCune, R. Andre, G. Bateman, and A. Kritz, Comput. Phys. Commun. **159**, 157 (2004).